SUPPLEMENTARY APPENDIX

Multi-parametric single cell evaluation defines distinct drug responses in healthy hematologic cells that are retained in corresponding malignant cell types

Muntasir M. Majumder,[1] Aino-Maija Leppä,[1] Monica Hellesøy,[2] Paul Dowling,[3] Alina Malyutina,[1] Reidun Kopperud,[4] Despina Bazou,[5] Emma Andersson,[6] Alun Parsons,[1] Jing Tang,[1] Olli Kallioniemi,[1,7] Satu Mustjoki,[6,8] Peter O'Gorman,[5] Krister Wennerberg,[1,9] Kimmo Porkka,[8,10] Bjørn T. Gjertsen[2,4] and Caroline A. Heckman[1]

[1]Institute for Molecular Medicine Finland FIMM, Helsinki Institute of Life Science, University of Helsinki, Helsinki, Finland; [2]Hematology Section, Department of Internal Medicine, Haukeland University Hospital, Bergen, Norway; [3]Department of Biology, National University of Ireland, Maynooth, Ireland; [4]Centre for Cancer Biomarkers CCBIO, Department of Clinical Science, University of Bergen, Bergen, Norway; [5]Department of Hematology, Mater Misericordiae University Hospital, Dublin, Ireland; [6]Department of Clinical Chemistry and Hematology, University of Helsinki, Finland; [7]Science for Life Laboratory, Department of Oncology and Pathology, Karolinska Institute, Solna, Sweden; [8]Hematology Research Unit Helsinki, University of Helsinki, Helsinki, Finland; [9]BRIC-Biotech Research and Innovation Centre, University of Copenhagen, Copenhagen, Denmark and [10]Department of Hematology, Helsinki University Hospital Comprehensive Cancer Center, Helsinki, Finland

©2020 Ferrata Storti Foundation. This is an open-access paper. doi:10.3324/haematol.2019.217414

Received: January 24, 2019.

Accepted: August 22, 2019.

Pre-published: August 22, 2019.

Correspondence: *CAROLINE A. HECKMAN*- caroline.heckman@helsinki.fi

MUNTASIR MAMUN MAJUMDER - muntasir.mamun@helsinki.fi

SUPPLEMENTARY INFORMATION

Multi-parametric single cell evaluation defines distinct drug responses in healthy hematologic cells that are retained in corresponding malignant cell types

Muntasir M. Majumder[1*], Aino-Maija Leppä[1], Monica Hellesøy[2], Paul Dowling[3], Alina Malyutina[1], Reidun Kopperud[2], Despina Bazou[4], Emma Andersson[5], Alun Parsons[1], Jing Tang[1], Olli Kallioniemi[1,6], Satu Mustjoki[5,7,8], Peter O'Gorman[4], Krister Wennerberg[1, 9], Kimmo Porkka[7,8], Bjørn T. Gjertsen[2], Caroline A. Heckman[1*]

Affiliations:

1. Institute for Molecular Medicine Finland FIMM, Helsinki Institute of Life Science, University of Helsinki, Helsinki, Finland
2. Hematology Section, Department of Internal Medicine, Haukeland University Hospital, and Centre for Cancer Biomarkers CCBIO, Department of Clinical Science, University of Bergen, Bergen, Norway
3. Department of Biology, National University of Ireland, Maynooth, Ireland
4. Department of Hematology, Mater Misericordiae University Hospital, Dublin, Ireland
5. Department of Clinical Chemistry and Hematology, University of Helsinki, Finland
6. Science for Life Laboratory, Department of Oncology and Pathology, Karolinska Institute, Solna, Sweden
7. Hematology Research Unit Helsinki, University of Helsinki, Helsinki, Finland
8. Department of Hematology, Helsinki University Hospital Comprehensive Cancer Center, Helsinki, Finland
9. BRIC- Biotech Research & Innovation Centre, University of Copenhagen, Copenhagen, Denmark

Running head: Innate drug responses in hematological cell populations

***Correspondence:**

Caroline A. Heckman, PhD
Institute for Molecular Medicine Finland (FIMM)
P.O. Box 20 (Tukholmankatu 8)
FI-00014 University of Helsinki, Finland
Phone: +358 29 412 5769
Email : caroline.heckman@helsinki.fi

Muntasir Mamun Majumder, PhD
Institute for Molecular Medicine Finland (FIMM)
P.O Box 20 (Tukholmankatu 8)
FI-00014 University of Helsinki, Finland
Phone: +358 40 3650837
Email : muntasir.mamun@helsinki.fi

TABLE OF CONTENTS

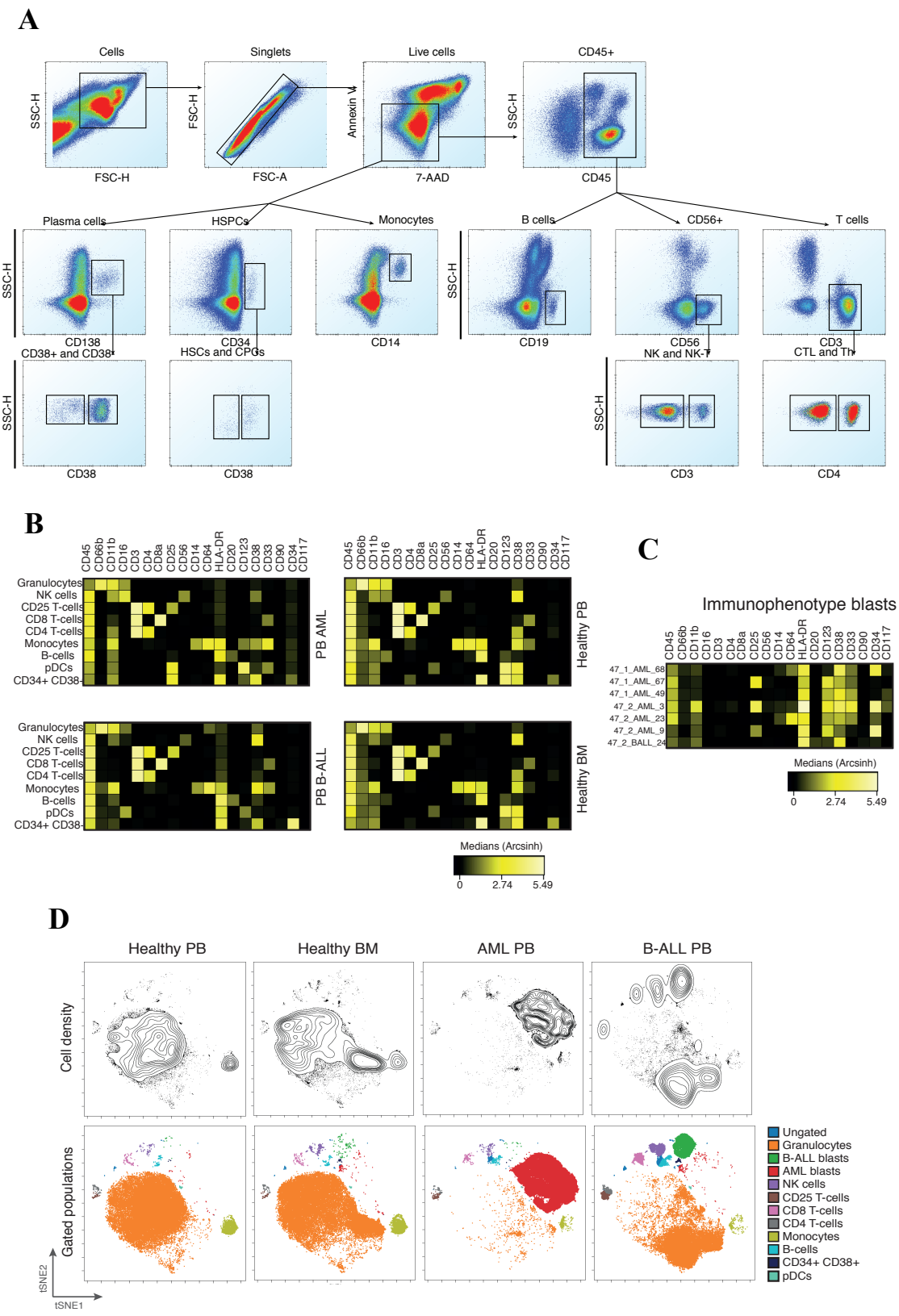

Supplementary Figure S1. Immunophenotyping of hematopoietic cell types based on their surface antigen expression applied in flow cytometry (A) and mass cytometry assay (B) and (C). (**A**) Gating strategy for flow cytometry assay. Briefly, singlet mononuclear cells were subjected to dead and apoptotic cell exclusion using DNA staining dye 7-AAD and expression of Annexin-V surface antigens. 11 cell subsets were detected based on the expression of their core surface antigens (hematopoietic stem cells (HSC/CD34+CD38-), common progenitor cells (CPC/CD34+CD38+),

monocytes/CD14+, B/CD45+CD19+, cytotoxic T/CD45+CD3+CD8+ cells, T helper/CD45+CD3+CD4+ cells, NK-T/ CD45+CD3+CD56+ cells, NK/ CD45+CD56+CD3-) cells, plasma cell subsets /CD138+CD38+ and CD138+CD38- and granulocytes/CD45^{low}, SSC++. (**B**) Immunophenotype of cell types and their corresponding antigen expression in specimens used in mass cytometry. (**C**) Immunophenotype of blast cells in analyzed AML samples. (**D**) Contour (upper panel) and overlaid scatter plot (lower panel) displaying gated cell lineages for Cohort IV samples used in mass cytometry analysis.

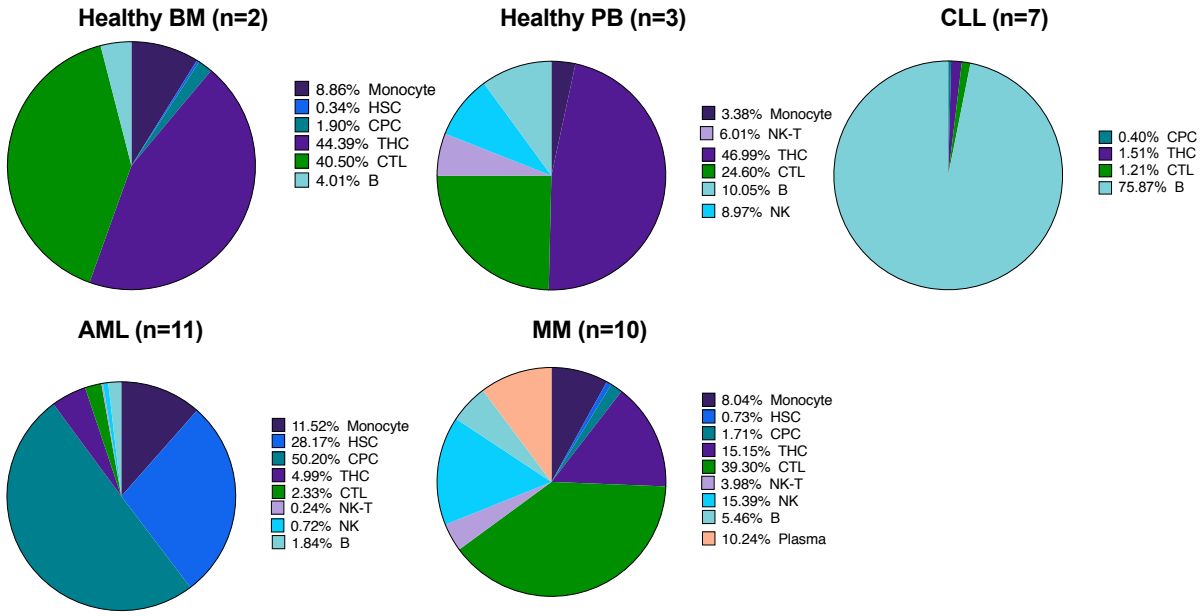

Supplementary Figure S2. Cellular composition of analyzed healthy and patient samples. Pie charts plotting the average proportions of different hematopoietic cell subpopulations detected in the analyzed samples with the numbers of each sample type indicated. Data from individual samples are provided in Supplemental Tables S3 and S4. The CD56 antibody was not included in the assessment of Cohort II samples, so proportions of NK and NK-T cells in healthy BM and CLL samples are not reported.

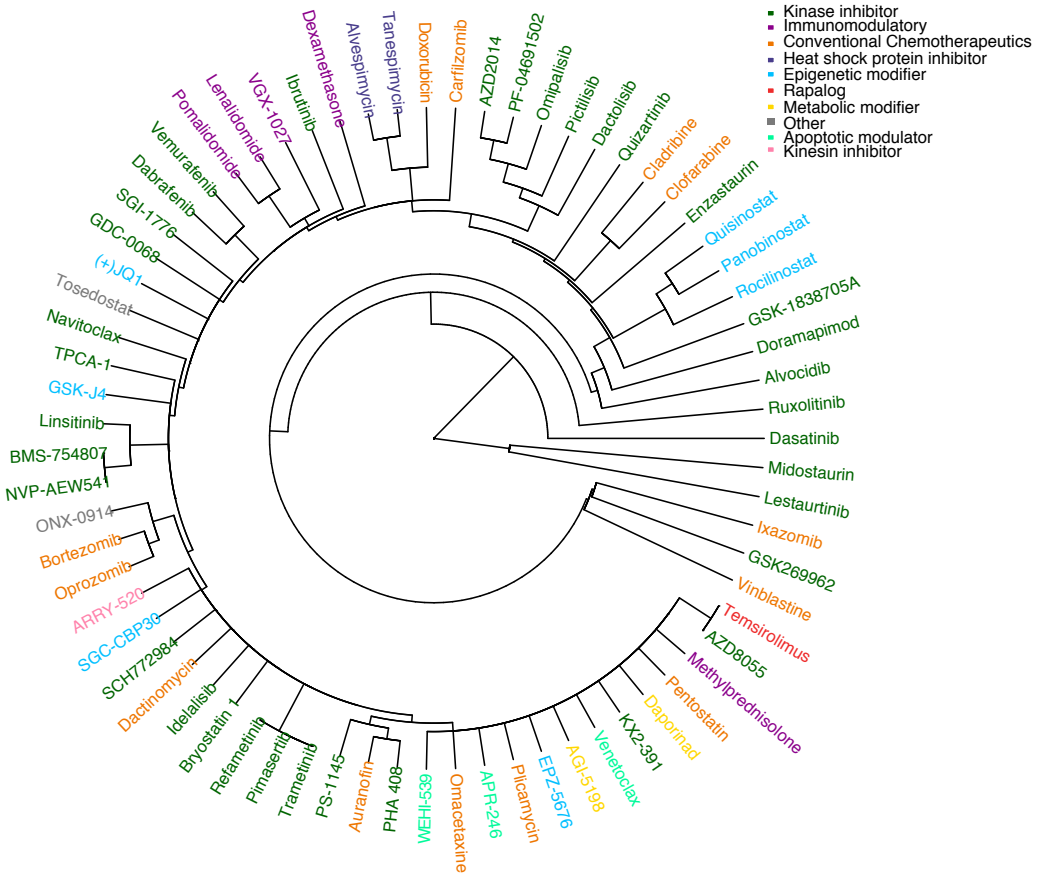

Supplementary Figure S3. Functional classes of 71 small molecules investigated for cell type specific activity. The 71 small molecules that were tested are clustered based on Spearman correlation of drug sensitivity scores derived from their effect on six hematopoietic cell subsets in three healthy PB samples. Drugs have been highlighted in distinct colors based on their primary mechanism of action. Annotations for the drug classes and assigned colors are located in the top right corner of the plot.

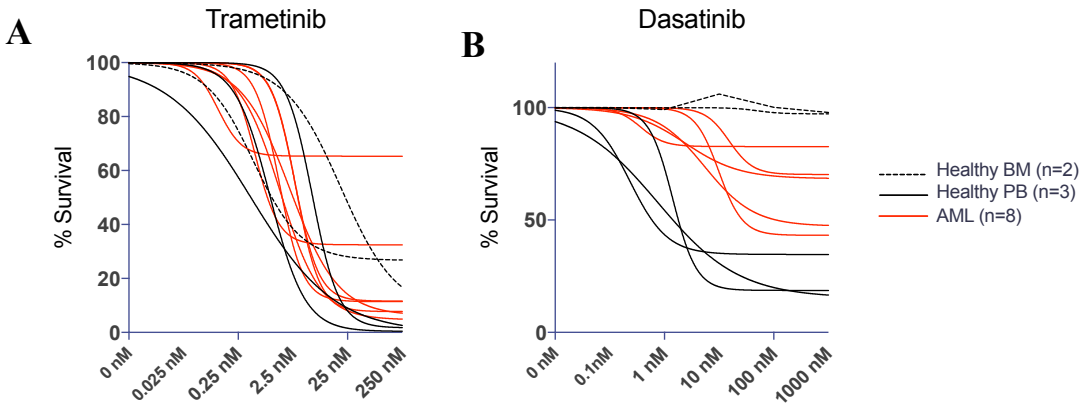

Supplementary Figure S4. Monocyte specific response to trametinib and dasatinib. Trametinib and dasatinib were tested in 14 samples (Cohort II) that included healthy PB (n=3), healthy BM (n=2),

AML (n=8) and CLL (n=3) samples. No CD14+ cells were detected in CLL samples and excluded from the graph. **(A)** Trametinib activity on monocytes was detected in all samples. **(B)** Higher sensitivity to dasatinib was noted in blood aspirates compared to BM samples from healthy individuals. CD14+ AML cells showed modest sensitivity.

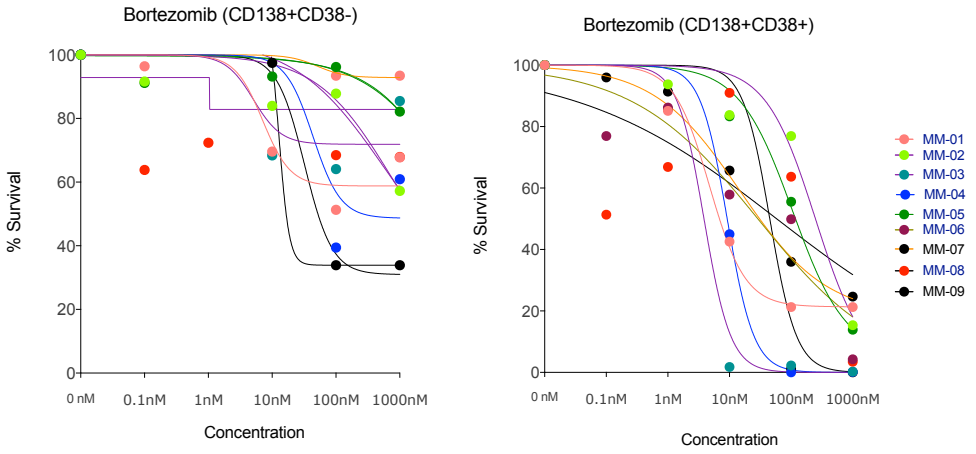

Supplementary Figure S5. Bortezomib response in plasma cell subsets. Sensitivity to bortezomib in two plasma cell subsets (CD138+CD38+ and CD138+CD38-) was compared in eight multiple myeloma (MM) samples. CD138+CD38- cells are less sensitive to bortezomib compared to CD138+CD38+ cells.

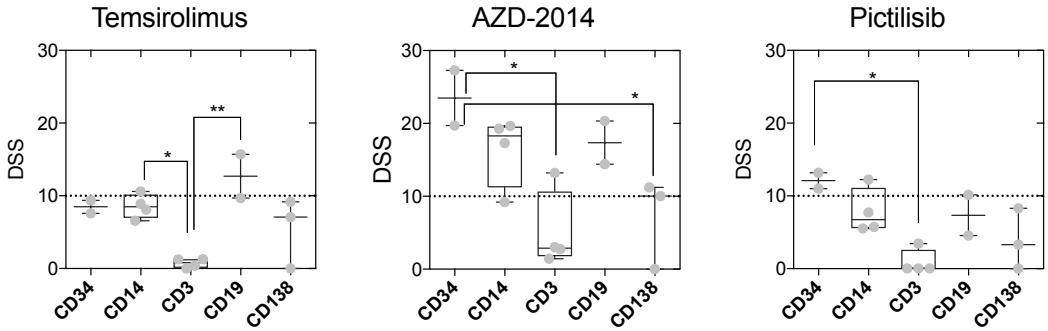

Supplementary Figure S6. T cell subsets are insensitive to PI3K-AKT-mTOR inhibitors compared to other immune cell subsets. CD34+, CD14+ and CD19+ are more sensitive to mTOR inhibitors. Data presented here show a comparison of drug sensitivity scores for temsirolimus (mTORC1 inhibitor), AZD-2014 (inhibits mTORC1 and mTORC2) and pictilisib (inhibits both PI3K and mTOR) between healthy cell types. Importantly, higher phosphorylation of mTOR signaling proteins (p4E-BP1 and pPLC-Y) was noted (Figure. 6).

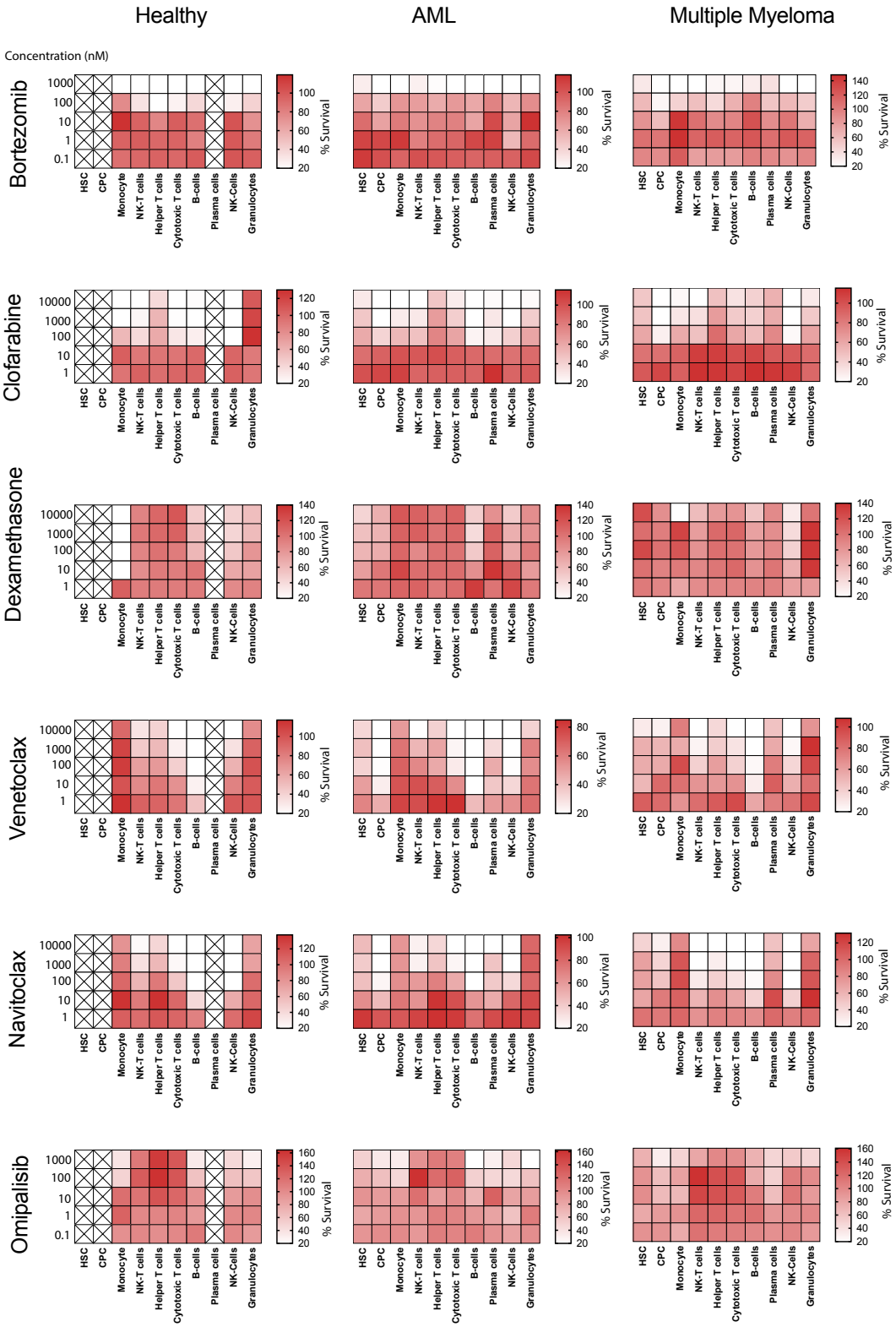

Supplementary Figure S7. **Lineage specificity of small molecules was observed in cells derived from healthy, AML and MM patients**. The data for six molecules presented here are organized in three rows for healthy, AML and MM samples. Viability of cells tested in five concentrations of the tested compounds is summarized in the heat maps. Concentrations for the drugs are displayed on the left side of the figure panels. HSC/CD34+CD38-, CPC/CD34+CD38+, monocyte/CD14+, natural killer-T/ CD3+CD56+, helper T/CD3+CD4+, cytotoxic T/CD3+CD4-, B/CD19+, natural killer/CD3-CD56+, granulocytes/CD45^{low}SSC++.

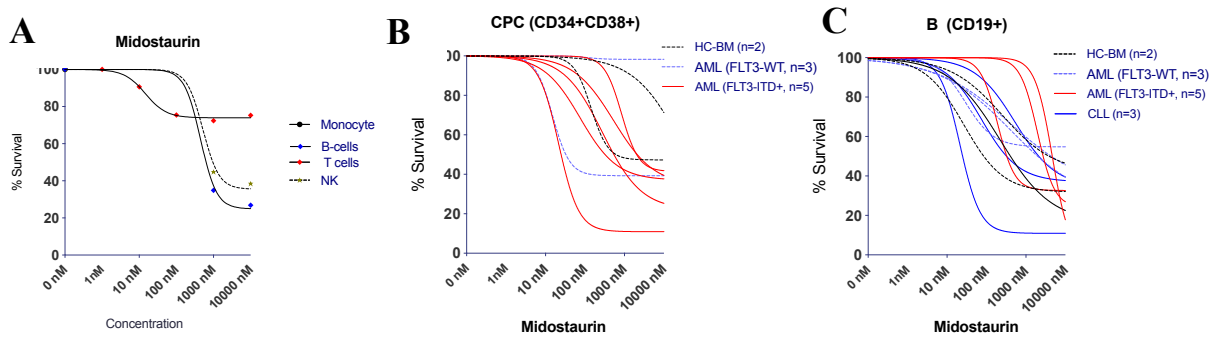

Supplementary Figure S8. Lineage specific activity of midostaurin. (**A**) B/CD19+ and NK/CD56+ cells are sensitive to midostaurin. (**B**) Response of committed progenitor cells (CPC; CD34+CD38+) to midostaurin. (**C**) CD19+ response was detected in 17 additional samples including 7 CLL samples (blue solid lines), which is also presented in Figure 4C.

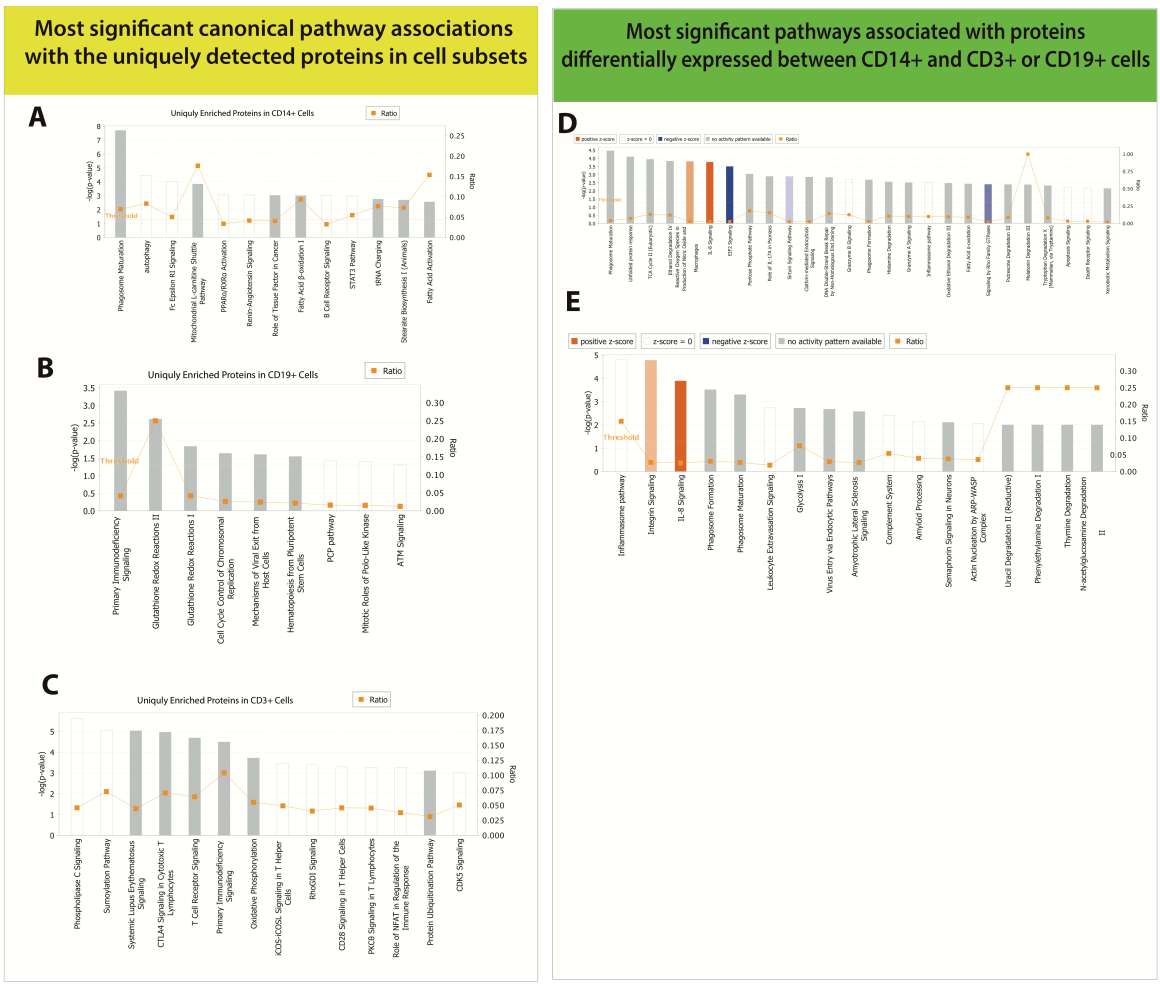

Supplementary Figure S9. Pathway enrichment analysis for unique and differentially expressed proteins detected in three healthy cell subsets (CD3+, CD14+ and CD19+cells). (**A-C**) A total of 163, 131 and 13 proteins were detected only in CD3+, CD14+ and CD19+, respectively. These proteins were analyzed using Ingenuity Pathway Analysis (IPA®, Qiagen). Significant pathways for CD14+ (**A**), CD19+ (**B**) and CD3+ (**C**) cells are depicted here. The left y axis shows –log(p) values for each pathway and right y axis displays the ratio of proteins (proteins in the dataset / total number of proteins in the canonical pathway) enriched in those pathways. (**D** and **E**) Enrichment of pathways

for proteins differentially expressed between CD14+ cells and CD3+ or CD19+ cells. Pathway enrichment was done for differentially expressed proteins between CD14+ versus CD3+ cells (**D**) and CD14+ versus CD19+ positive cells (**E**) (false discovery rate < 0.05). Highlighted red and blue bars represent activated or inhibited pathways in CD14+ cells compared to CD3+ or CD19+ cells.

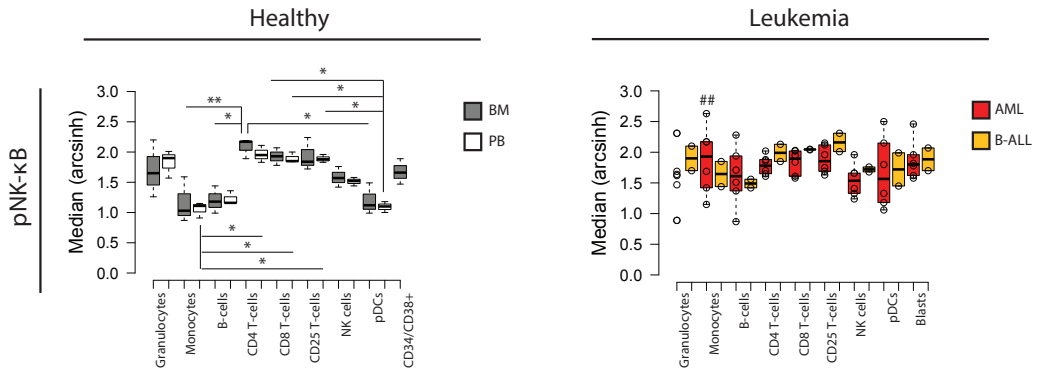

Supplementary Figure S10. Higher basal phosphorylation of NF-κB was detected in CD4+ and CD8+ T cells compared to other cell types. Phosphorylation was measured by mass cytometry and presented as median arcsinh values. Box plot representation of population medians of pNF-κB in healthy PB and BM (left) and leukemic samples (right). Center lines of boxes show medians; box limits indicate the 25th and 75th percentiles as determined by R software; whiskers extend 1.5 times the interquartile range from the 25th and 75th percentiles, outliers are represented by dots; data points are plotted as open circles. * Indicates significant difference (two-way ANOVA, Tukey's HSD) between all corresponding populations, unless specified as not significant (ns). # Indicates significance between AML and the corresponding healthy populations in both PB and BM. There were no significant differences between PB and BM in any populations or phosphorylation levels. *p<0.05, **p<0.005, ***p<0.0005.

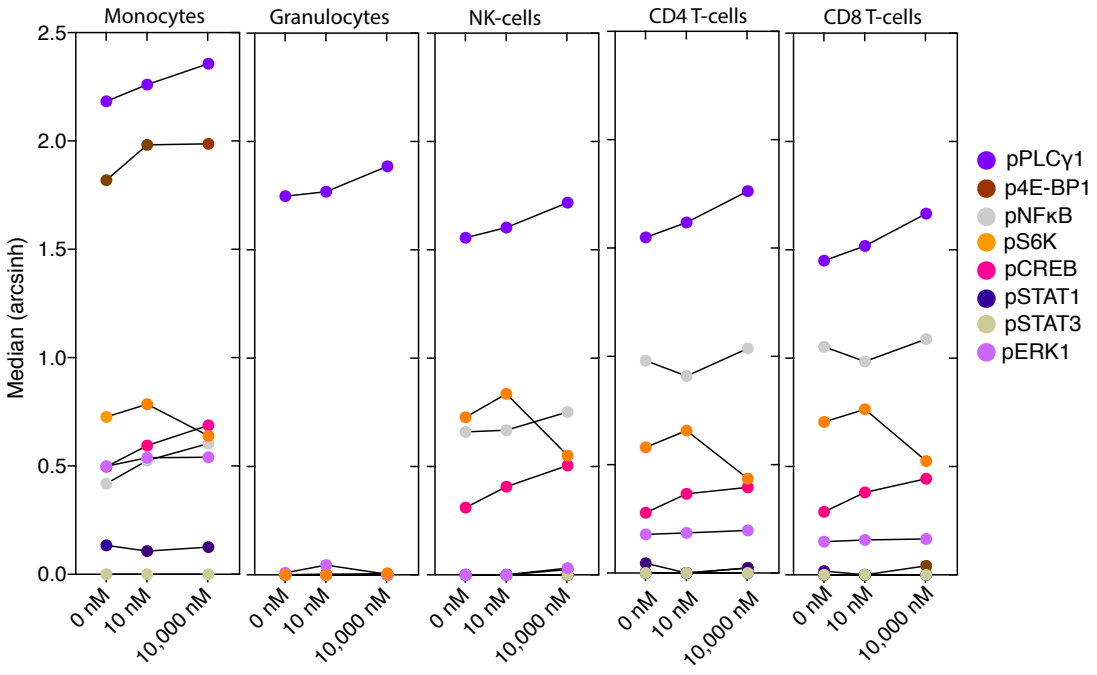

Supplementary Figure S11. Changes in signaling patterns across cell types with increasing concentrations of venetoclax. To understand how drug treatment might affect the signaling behavior at the single cell level we treated three PB MNCs with 0.10 and 10,000 nM of venetoclax and incubated for 30 minutes before fixation. Experimental conditions for mass cytometry were consistent with the earlier analysis for detection of basal signaling as described in the Methods section and with results shown in Figure 6. Antibody panels and immunophenotypic details are similar to what we described in Supplementary Table S1 and Supplementary Figure S1B. Results are presented as median arcsinh in the y axis and the x axis indicates the different concentrations of venetoclax that were tested.

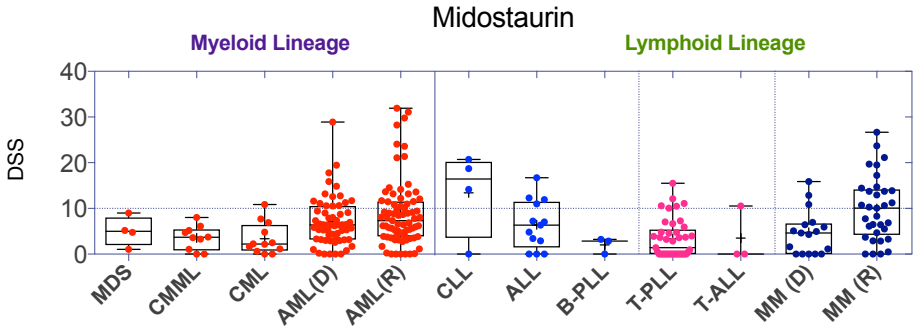

Supplementary Figure S12. Midostaurin shows efficacy in chronic and acute lymphocytic leukemia. Drug responses presented as DSS scores are compared across disease types in a cohort of 281 primary samples. Midostaurin response was detected in healthy B cells, CLL and ALL samples.

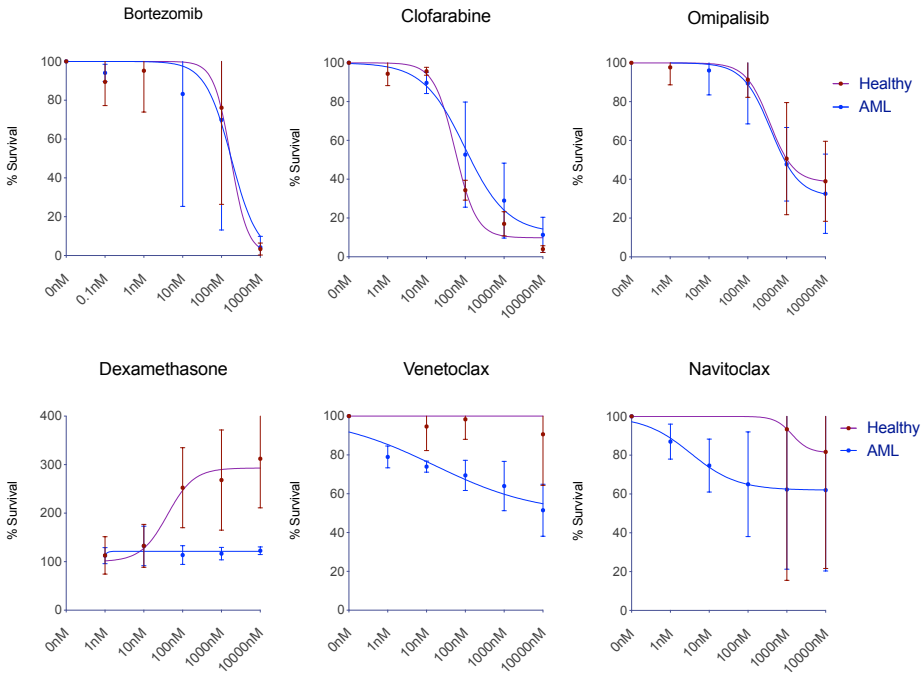

Supplementary Figure S13. Cellular effect of six indexed drugs on healthy and AML derived CD14+ cells. Dose response curves presented as mean ± SEM responses indicate similar responses observed for the three drugs shown in the upper panel. In the lower panels, AML CD14+ cells show modest sensitivity to venetoclax and navitoclax compared to healthy CD14+ cells.

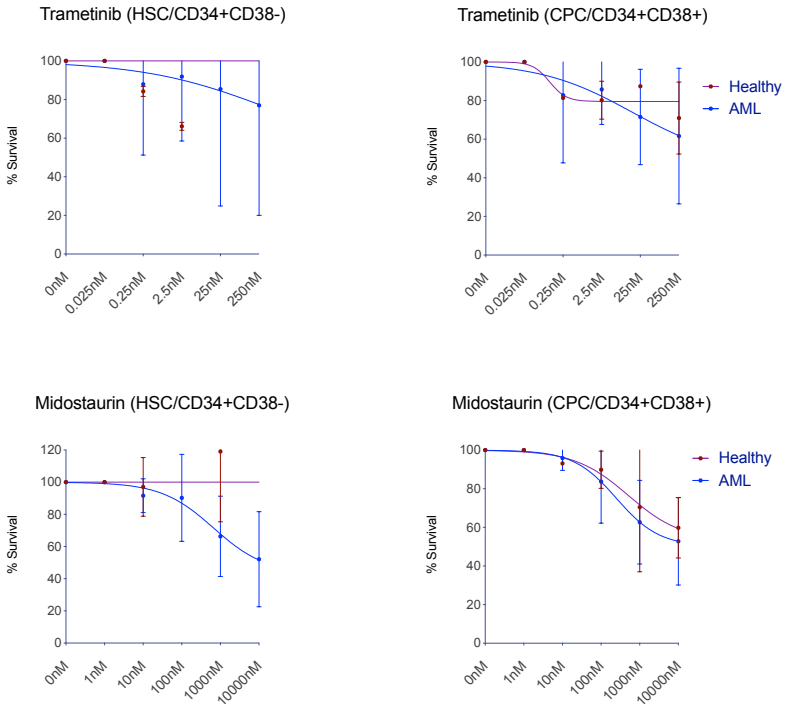

Supplementary Figure S14. Cellular effect of trametinib and midostaurin on healthy and AML derived HSC/CD34+CD38- and CPC/CD34+CD38+ cells. Uncommitted hematopoietic stem cells (HSC; CD35+CD38-) and committed progenitor cells (CPC; CD34+CD38+) from healthy donors and AML patients show similar responses to trametinib. However, AML derived CD34+CD38- cells appeared to be more sensitive to midostaurin compared to healthy HSC.

Supplementary Table S1. Antibody panels for flow cytometry and CyTOF assays

	Panel	Antibody	Clone	Fluorophore	Channel	Catalogue number
Cohort I	I	CD38	LD38	FITC	BL1	CYT-38F
		CD34	8G12	PE-Cy7	BL5	348811
		CD14	M5E2	BV786	VL6	563698
		CD138	MI15	APC	RL1	347216
		CD9	M-L13	APC-H7	RL1	655409
		Annexin V	-	PE	BL2	556422
		7-AAD	-	-	BL4	559925
	II	CD38	LD38	FITC	BL1	CYT-38F
		CD56	REA196	PE-Vio770	BL5	130-100-676
		CD3	SK7	APC	BL4	345767
		CD4	RPA-T4	BV421	VL1	562424
		CD19	SJ25C1	BV510	VL2	562947
		CD45	HI30	BV786	VL6	563716
		Annexin V	-	PE	BL2	556422
		7-AAD	-	-	BL4	559925
	III	CD56	REA196	PE-Vio770	BL5	130-100-676
		CD3	SK7	APC	RL1	345767
		CD4	RPA-T4	BV421	VL1	562424
		CD19	SJ25C1	BV510	VL2	562947
		CD45	HI30	BV605	VL4	564047
		CD14	M5E2	BV786	VL6	563698
		Annexin V	-	PE	BL2	556422
		7-AAD	-	-	BL4	559925
Cohort II	IV	CD38	LD38	FITC	BL1	CYT-38F
		CD34	8G12	Pe-Cy7	BL5	348811
		CD14 APC	M5E2	APC	RL1	561383
		CD4 BV421	SJ25C1	BV21	VL1	562424
		CD19	SJ25C1	BV510	VL2	562947
		CD3	SK7	BV605	VL4	563219
		CD45	HI30	BV786	VL6	563716
		Annexin V	-	PE	BL2	556422
		7-AAD	-	-	BL4	559925

	Panel	Antibody	Clone	Metal tag	Vendor	Catalogue number
Cohort IV	V	**Barcodes**				
		MBC #1		102 Pd	Fluidigm	201060
		MBC #2		104 Pd	Fluidigm	
		MBC #3		105 Pd	Fluidigm	
		MBC #4		106 Pd	Fluidigm	
		MBC #5		108 Pd	Fluidigm	
		MBC #6		110 Pd	Fluidigm	
		Surface panel				
		CD45	Hi30	89 Y	Fluidigm	3089003B
		CD66b	G10F5	141 Pr	BioLegend	305102
		CD117 (cKit)	104D2	143 Nd	Fluidigm	3143001C
		CD38	HIT2	144 Nd	Fluidigm	3144014C
		CD4	RPA-T4	145 Nd	Fluidigm	3145001B
		CD64	10.1	146 Nd	Fluidigm	3146006C
		CD20	2H7	147 Nd	Fluidigm	3147001B
		CD16	3G8	148 Nd	Fluidigm	3148004B
		CD123 (IL-3R)	6H6	151 Eu	Fluidigm	3151001B
		CD56 (NCAM)	B159	155 Gd	Fluidigm	3155008B
		CD90 (Thy-1)	5E19	159 Tb	Fluidigm	3159007C
		CD14	M5E2	160 Gd	Fluidigm	3160001B
		CD8a	RPA-T8	162 Dy	Fluidigm	3162015C
		CD33	WM53	163 Dy	Fluidigm	3163023B
		CD34	581	168 Er	BioLegend	343531
		CD25 (IL-2R)	2A3	169 Tm	Fluidigm	3169003C
		CD3	UCHT1	170 Er	Fluidigm	3170001B
		HLA-DR	L243	174 Yb	Fluidigm	3174001C
		CD11b (Mac-1)	Mac-1	209 Bi	Fluidigm	3209003B
		Intracellular panel				
		p-4E-BP1 (T37/46)	D3E9	142 Nd	Fluidigm	3142004C
		pAkt (S473)	47	150 Nd	Fluidigm	3150005A
		pSTAT1 (Y701)	D9E	152 Sm	Fluidigm	3152005C
		pSTAT3 (Y705)	D3F9	156 Gd	Fluidigm	3156002C
		pCREB (S133)	713610	161 Dy	R&D Systems	CFNY041609
		pNFkB (S529)	87G3	165 Ho	Fluidigm	3165009A
		pErk1/2	K10-895.12.50	166 Er	Fluidigm	3166006A
		(T202/Y204)	D1314.4E	167 Er	Fluidigm	3167005C
		pS6 (S235/236)	N7-548	172 Yb	Fluidigm	3172008A
		pPLCg1 (Y783)	12F4.2	176 Yb	Millipore Sigma	2752567

Supplementary Table S3. Cellular proportions of cohort-I samples. Values are presented as percentage ratio of count of events for individual populations compared to live cells

		Cohort-I														
		Healthy PB			Multiple Myeloma									AML		
Cell Types		HC-1	HC-2	HC-3	MM-1862	MM-933	MM-3821	MM-4296	MM-828	MM-4312	MM-5704	MM-870	MM-3001	AML-5750	AML-4634	AML-4701
Plasma	**CD138+**				7,07	3,07	14,76	0,83	1,53	12,41	0,70	2,88	3,45			
Monocyte	**CD14+**	2,55	2,56	1,76	12,89	2,48	2,65	5,02	0,97	3,86	1,00	6,28	1,50	2,84	2,52	2,94
HPC	**CD34+CD38-**		-		1,68	0,07	0,41	0,11	0,05	0,06	0,33	0,23	0,39	0,42	4,22	3,19
CPC	**CD34+CD38+**		-		4,80	0,14	0,21	0,54	0,13	0,21	0,64	0,69	0,46	79,40	20,51	29,84
THC	**CD3+CD4+**	36,84	30,77	27,85	2,03	7,49	11,65	8,28	13,60	6,54	11,16	3,48	4,87	0,63	2,16	2,08
CTL	**CD3+CD8+**	23,02	16,49	10,47	0,95	1,02	26,82	43,37	39,40	39,88	17,14	8,77	1,89	0,81	3,33	2,82
NK-T	**CD56+CD3+**	0,88	10,73	0,61	0,30	0,60	1,80	0,90	4,50	3,28	4,58	0,30	1,88	0,08	0,20	0,23
NK	**CD56+CD3-**	3,85	8,36	6,01	1,35	2,57	31,06	6,57	6,10	14,18	0,85	7,37	0,16	0,18	1,35	0,03
B	**CD19+**	8,13	11,97	0,31	0,01	3,32	4,16	4,67	3,30	5,04	3,42	0,17	0,81	0,56	4,47	0,46

Supplementary Table S4. Mean IC50 and R2 (curve fitting) values for venetoclax organized according to cell types and disease categories (associated with Figure 3B)

Venetoclax			
Cell Type	**Samples**	**Mean IC50 (M)**	**Mean R2**
CD19+	Healthy (PB, n=3)	4.228E-09	0.9861
	AML (n=3)	8.469E-10	0.9947
	Myeloma (n=10)	5.67E-09	0.9817
CD56+	Healthy (PB, n=3)	1.324E-07	0.9823
	AML (n=3)	5.73E-09	0.9947
	Myeloma (n=10)	7.118E-09	0.9772
CD3+CD4+	Healthy (PB, n=3)	1.103E-06	0.933
	AML (n=3)	8.33E-09	0.8837
	Myeloma (n=10)	3.062E-08	0.9799
CD3+CD4-	Healthy (PB, n=3)	3.422E-08	0.9849
	AML (n=3)	7.405E-09	0.9704
	Myeloma (n=10)	2.131E-08	0.9194
CD3+CD56+	Healthy (PB, n=3)	2.674E-07	0.8481
	AML (n=3)	9.975E-07	0.8514
	Myeloma (n=10)	3.268E-08	0.9507

Supplementary Table S5. Cellular proportions of Cohort II samples. Values are presented as percentage ratio of count of events for individual populations compared to live cells. **Anti CD56 antibody was not included in the assay and the proportion could not be measured in those samples.*

		Cohort-II																
		Healthy BM		AML-FLT3-WT			AML-FLT3-ITD					CLL						
Cell Types		HC-BM-1	HC-BM-2	AML-6641	AML-4654	AML-4361	AML-5237	AML-6545	AML-1886	AML-3853	AML-4453	CLL-4098_2	CLL-4490	CLL-4593	CLL-224	CLL-4098_3	CLL-4375	CLL-1829
Plasma	**CD138+**																	
Monocyte	**CD14+**	1,91	6,32	13,73	14,27	15,69	11,56	10,57		3,13	5,17							
HPC	**CD34+CD38-**	0,06	0,26	14,28	31,12	16,19	71,39	26,71	12,02	22,08	20,12							
CPC	**CD34+CD38+**	0,29	1,47	36,45	17,90	22,16	13,06	31,29	29,81	52,88	61,79	0,05	0,05	1,16	0,07	0,02	0,28261	0,556242
THC	**CD3+CD4+**	26,98	14,24	4,84	16,70	5,69	2,43	1,09	1,27	1,39	0,95	1,11	2,22	2,41	1,05	0,67	0,131885	0,605686
CTL	**CD3+CD8+**	22,25	15,35	1,73	3,45	2,76	0,87	0,36	1,03	0,57	0,59	0,13	0,68	3,53	0,41	0,13	0,27005	1,421508
NK-T*	**CD56+CD3+**																	
NK*	**CD56+CD3-**																	
B	**CD19+**	1,74	1,99	1,25	1,63	2,34	1,17	1,11	0,97	0,12	0,42	95,09	83,97	61,55	76,12	90,35	57,67129	60,35847

Supplementary Table S6: Mean IC50 and R2 (curve fitting) values for midostaurin organized according to cell types and disease categories (associated with Figure 4A-C)

Midostaurin			
Cell Type	**Samples**	**Mean IC50 (M)**	**Mean R2**
HSC (CD34+CD38-)	Healthy (BM, n=2)	NA	0.7065
	AML-FLT3-WT (n=3)	8.914E-07	0.9931
	AML-FLT3-ITD (n=5)	2.621E-07	0.9813
	CLL (n=7)	NA	NA
CPC (CD34+CD38+)	Healthy (BM, n=2)	0.000000189	0.811
	AML-FLT3-WT (n=3)	5.116E-08	0.7203
	AML-FLT3-ITD (n=5)	1.255E-07	0.7918
	CLL (n=7)	NA	NA
B (CD19+)	Healthy (BM, n=2)	5.766E-08	0.9914
	AML-FLT3-WT (n=3)	9.65E-08	0.9412
	AML-FLT3-ITD (n=5)	0.000001959	0.9266
	CLL (n=7)	4.504E-08	0.9929

SUPPLEMENTARY METHODS

Optimization of the no wash high-throughput flow cytometry assay and antibody panels for drug sensitivity and functional assessment of cell subsets

We have optimized a no wash assay that allowed us to simultaneously monitor drug responses in immune subsets using a high throughput (HT) flow cytometer (iQue®Screener PLUS). The assay enables screening of small molecules capable of inducing apoptosis, monitoring their immune effects, and to predict off target effects due to cell subset selectivity. Assay optimization was carried out with human samples to identify optimal cell density, antibody dilutions, incubation time, and finally to compare staining performances with and without washing. The cell culture medium used for all assays was comprised of RPMI 1640 medium supplemented with 10% fetal bovine serum, 2 mM L-glutamine, penicillin (100 U/ml), streptomycin (100 µg/ml) and 25% conditioned medium from the HS-5 human BM stromal cell line. BM samples were seeded at 0.5, 1, 2 and 4 million per ml density to compare effect on drug responses for 5 small molecules (**Figure A**) at 72 hours. A density of 2 million cells/mL was selected for the assay. Next, we tested in serial dilutions from the recommended concentration (1:24,1:48,1:96,1:192 and 1:384) to identify the optimal signal to noise ratio for each antibody (**Figure B**).

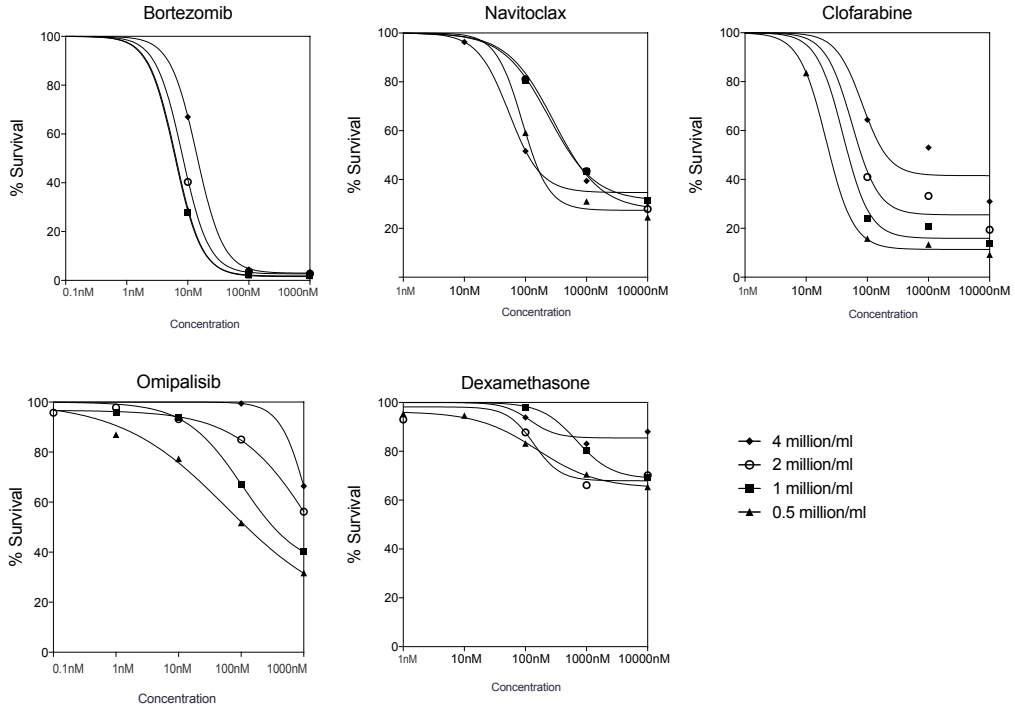

Figure A. **Effect of cell density on response to specific drugs**. The effect of five indexed drugs was measured at different cell densities ranging from 0.5-4 million cells/mL. The x axis displays percentage of cells viable compared to untreated controls (DMSO) tested in five concentrations as displayed in the y axis.

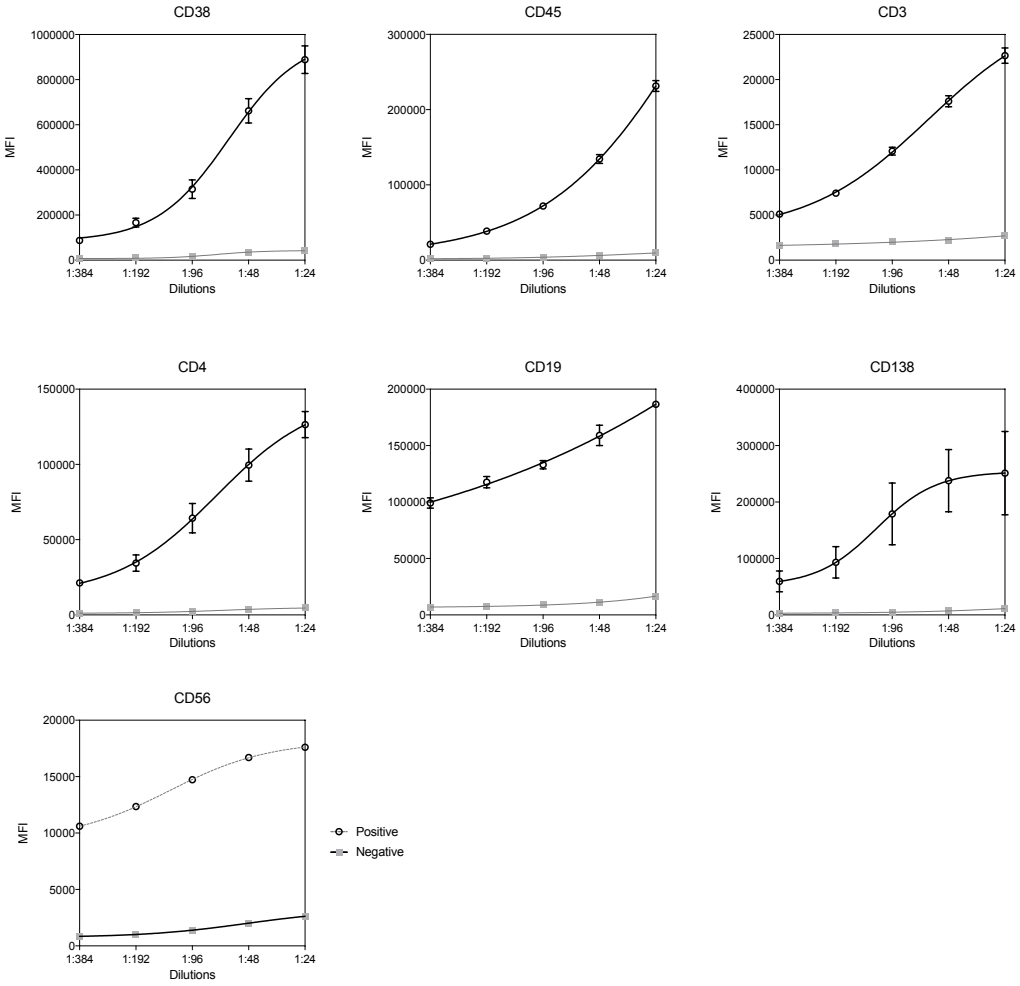

Figure B. **Assessment of signal to noise ratio to identify the optimum dilutions for each antibody**. CD38, CD45, CD3, CD4, CD19, CD138 antibodies were tested with BM cells from five myeloma patients. The antibodies were diluted in ratios of 1:24, 1:48, 1:96, 1:192 and 1:384 from the original antibody stock. The CD56 antibody was tested using a single sample. Concentrations for other antibodies were derived from prior experience and optimization experiments, which are not described here.

The following mAbs were purchased from BD Biosciences: APC anti-CD3 (clone SK7), BV421 anti-CD4 (clone RPA-T4), BV510 anti-CD19 (clone SJ25C1), BV786 anti-CD45 (clone HI30), PE-Cy7 anti-CD34 (clone 8G12), APC anti-CD138 (clone MI15), APC-H7 anti-CD9 (clone M-L13), BV786 anti-CD14 (clone M5E2), PE Annexin-V and 7-amino-actinomycin (7-AAD). The mAb FITC anti-CD38 (clone LD38) was purchased from Cytogonos and the mAb PE-Vio770 anti-CD56 (clone REA196) was purchased from Miltenyi Biotec. Compensation was carried out with the final titration for the designed panels.

To compare wash versus no wash methods, we used the brilliant violet dye CD45 BD-786. A 1:1 ratio dilution with staining buffer (PBS with 0.5% bovine serum albumin) was able to reasonably discriminate positively and negatively stained cell populations in the no wash assay as compared to cells undergoing wash steps after the addition of antibodies.

An incubation of one hour was found ideal for the constructed panel (data not shown). Two samples were tested with fresh cells and with viable cryopreserved cells to compare the effect of freezing and thawing on antigen stability (data not shown).

Flow cytometric analysis of drug response was performed in both 384 well plates (n=4) with 71 drugs and 96 well plates (n=15) with 6 drugs. Cellular response was measured after 72 hours incubation. In the 96 well plates, the antibodies were tested in two panels to study the effects of 6 drugs in 5 dilutions (1-10000 nM) (clofarabine, bortezomib, dexamethasone, navitoclax, venetoclax and omipalisib) on 11 cell populations, namely hematopoietic stem cells (HSCs; CD34+CD38-), common progenitor cells (CPCs; CD34+CD38+), monocytes (CD14+), B cells (CD45+CD19+), cytotoxic T cells (CD45+CD3+CD8+), T helper cells (CD45+CD3+CD4+), NK-T cells (CD45+CD3+CD56+), NK cells (CD45+CD56+CD3-), clonal plasma cells (CD138+CD38+), other plasma cells (CD138+CD38-) and granulocytes ($CD45^{low}$, SSC++). These compounds showed differential response across cell types in the primary screen with 71 compounds. Annexin-V and 7AAD were used to distinguish live cell populations from apoptotic and dead cells. Additionally, frozen viable cells from FLT3-ITD positive AML (n=3) and CLL (n=7) has been tested with midostaurin, dasatinib and trametinib along with fresh BM samples from healthy individuals on 7 cell populations.

After 1 h incubation with antibodies, the plates were read with the iQue® Screener PLUS instrument (Intellicyt). Data were analyzed using ForeCyt software (Intellicyt). Counts for each population were used to generate four parameter nonlinear regression fitted dose response curves with GraphPad Prism 7. Three samples were tested in duplicate to assess reproducibility. To assess cell viability or antigen stability during 3 days incubation, we compared the normalized count for each cell type relative to live cells processed at 0 and 72 hrs.